# Enhanced activity for supported Au clusters: Methanol oxidation on Au/TiO2(110)

**ARTICLE** *in* SURFACE SCIENCE · AUGUST 2012

Impact Factor: 1.93 · DOI: 10.1016/j.susc.2012.04.002

Surface Science 606 (2012) 1233–1243

Contents lists available at SciVerse ScienceDirect

Surface Science

journal homepage: www.elsevier.com/locate/susc

# Enhanced activity for supported Au clusters: Methanol oxidation on Au/$TiO_2$(110)

Samuel A. Tenney, Brett A. Cagg, Mara S. Levine, Wei He, Kedar Manandhar, Donna A. Chen *

*Department of Chemistry and Biochemistry, University of South Carolina, Columbia, SC 29208, United States*

ARTICLE INFO

*Article history:*
Received 1 December 2011
Accepted 4 April 2012
Available online 23 April 2012

*Keywords:*
Temperature programmed desorption
Scanning tunneling microscopy
X-ray photoelectron spectroscopy
Au nanoparticles
Titania

ABSTRACT

Gold clusters supported on $TiO_2$(110) exhibit unusual activity for the oxidation of methanol to formaldehyde. Temperature programmed desorption studies of methanol on Au clusters show that both Au and titania sites are necessary for methanol reaction. Isotopic labeling experiments with $CD_3OH$ demonstrate that reaction occurs via O–H bond scission to form a methoxy intermediate. When the $TiO_2$ surface is oxidized with $^{18}O_2$ before or after Au deposition, methanol reaction produces $H_2^{18}O$ below 300 K, indicating that oxygen from titania promotes O–H bond scission and is incorporated into desorbing products. XPS experiments provide additional evidence that during methanol reaction on the Au/$TiO_2$ surface, methanol adsorption occurs on $TiO_2$, given that the titania support becomes slightly oxidized after exposure to methanol in the presence of Au clusters. While the role of $TiO_2$ is to dissociate the O–H bond and form the reactive methoxy intermediate, the role of the Au sites is to remove hydrogen from the surface as $H_2$, thus preventing the recombination of methoxy and hydrogen to methanol. The decrease in formaldehyde yield with increasing Au coverage above 0.25 ML suggests that reaction occurs at Au–titania interfacial sites; scanning tunneling microscopy images of various Au coverages confirm that the number of interfacial sites at the perimeter of the Au clusters decreases as the Au coverage is increased between 0.25 and 5 ML.



## 1. Introduction

Recently there has been great interest in the catalytic properties of Au nanoclusters for low temperature oxidation [1–10] and epoxidation [11] reactions. Despite the inertness of bulk Au surfaces, Au nanoclusters supported on titania have excellent selectivity for the low temperature epoxidation of propene with $O_2$, [11]. One of the major challenges in catalysis today is the development of a heterogeneous catalyst for the direct epoxidation of propene to propene oxide using molecular oxygen, given that propene oxide is a starting material for many organic synthesis products and represents a multibillion dollar industry for the production of 3.5 million tons of propene oxide/year [12,13]. Furthermore, Au nanoclusters on titania and other reducible metal oxide supports are known to be good catalysts for the low temperature oxidation of CO to $CO_2$ [2–6,14,15]. The ability to oxidize CO at low temperature is especially important for fuel cell applications [16–18] and for CO removal in automobile engines under cold start conditions [19] because the current automotive catalysts are not effective below 200 °C [20].

The surprising activity of titania-supported Au nanoclusters of less than 40 Å in diameter compared to the inactive bulk Au surfaces has been a topic of much discussion in the literature [8,10,21]. In particular, there have been many studies of CO oxidation on supported Au clusters, but the origins of the increased activity for the Au nanoclusters are not completely understood and are still a topic of controversy. Many factors are reported to influence the activity of the Au clusters, including electronic effects [22], interactions with the support [23–26], particle size [22,25,27–29], the nature of sites at the particle surface [31,39], the oxidation states of Au [6,32,33], the method of catalyst preparation [5] and the amount of residual chloride from the Au precursor [15].

Density functional theory (DFT) studies provide strong evidence that the unusual activity of the small Au clusters is due to the greater number of active, undercoordinated Au atoms at the surfaces of the clusters [31,39]. There is also good evidence that for reactions like CO oxidation, the enhanced activity of Au clusters on titania stems from the unique geometries of atoms on the cluster surfaces. DFT studies of supported Au clusters by the Norskov group have demonstrated that undercoordinated Au atoms on the Au clusters play an important role in the CO oxidation activity [31,34–40]. Activity of the clusters scales with the fraction of low coordination number Au atoms rather than the surface area of the clusters [31,36,37]. The binding energy of CO, atomic O and $O_2$ all decrease linearly with increasing coordination number of the Au atoms [36,41], and CO adsorption properties [28], as well as $O_2$ dissociation [38], are dominated by the activity of the undercoordinated Au atoms. Thus, activity of the small particles arises from the high fraction of atoms with special geometries, such as corner and edge atoms, rather than from their intrinsic size [36,39]. There are also experimental studies of Au on metal oxide supports that corroborate the idea that the unusual activity of the clusters can be explained by the high fraction of undercoordinated atoms with special geometries like corner and edge sites [42–44].

* Corresponding author. Tel.: +1 803 777 1050; fax: +1 803 777 9521.
*E-mail address:* dachen@sc.edu (D.A. Chen).

0039-6028/$ – see front matter © 2012 Elsevier B.V. All rights reserved.
doi:10.1016/j.susc.2012.04.002

While the importance of undercoodinated Au atoms is generally accepted, conflicting reports exist in the literature regarding the effects of cationic Au, the potentially unique activity of two-layer Au clusters, and the role of the support. For example, it has been proposed that cationic Au at the edges of the clusters is responsible for the enhanced CO oxidation activity. Gates and co-workers showed that for MgO-supported Au catalysts prepared from a Au(III) complex, the catalyst was more active when there was a higher concentration of Au(I) compared to metallic Au [32]. In contrast, Goodman and co-workers have investigated Au clusters vapor-deposited on crystalline titania surfaces and found that the presence of cationic Au is not an important factor in the enhanced activity of the clusters [45,46]. The Goodman group also reported that bilayer Au clusters on $TiO_2$ had significantly higher activity for CO oxidation than monolayer clusters or more three-dimensional Au clusters [45,47]. Furthermore, a STEM study of Au on $FeO_x$ catalysts showed that high activities were correlated with the presence of bilayer clusters of 0.5 nm in diameter [48]. However, the presence of bilayer clusters was not necessary for high activity of Au on an iron oxide support [49].

There is also compelling evidence that the Au–titania interface and associated active sites play an important role. Au clusters on highly reducible supports like ceria, titania and iron oxide exhibit higher activity than on nonreducible supports like AgO, alumina and silica [14,50], even for clusters of the same size range [51], and Au on $TiO_2$ is 2–3 times more active than Au on $SiO_2$ for CO oxidation [52–54]. Indeed, it has been proposed that both oxidation [4,55] and epoxidation [11,56,57] occur at the interface between the perimeter of the Au clusters and the titania support. Titania layers grown on inactive Au powder with 10 μm crystallites have high activity for CO oxidation, similar to the 3.5 nm Au particles on titania [53,54,58]; a study of titania clusters grown on Au(111) further demonstrates that the Au–titania interfacial sites are the active sites since this surface has the same activity for the water gas shift reaction as Au clusters grown on titania [59]. In addition, hemispherically shaped Au clusters on titania show greater activity for CO oxidation than spherically shaped clusters, and the increase in activity is attributed to the greater contact area between the support and the hemispherical clusters [2,6,60]. DFT [55] and experimental investigations [25] also report that the Au–titania interfacial sites are the active sites for CO oxidation, and in the proposed mechanism, CO is adsorbed on Au while $O_2$ is activated on titania. A similar mechanism was suggested for Au clusters on $Fe_2O_3$, which is another highly reducible support [50]. Moreover, DFT calculations indicate that the active surface species is bound to both the Au cluster and the support [38,61,62]. Recent work by the Yates group shows that the dissociation of $O_2$ occurs at the Au–titania interface via the formation of a CO–$O_2$ complex, and therefore reaction occurs at the perimeter of the clusters [63].

In other cases, the support is believed to play only a minor, secondary role [14]. For Au clusters on $TiO_2$, $MgAl_2O_4$ and $Al_2O_3$ supports, the differences in activity could be explained by the number of low coordination sites in the clusters, based on particle sizes measured in STEM and EXAFS as well as a geometric calculation; it was therefore not necessary to invoke particle–support interactions to explain enhanced activities [44]. DFT investigations report that the interfacial energy between the Au cluster and support determines the cluster dispersion, shape and structure, which in turn influences the number of active, low coordination Au sites [37]. For Au clusters vapor-deposited on crystalline titania, oxygen vacancy defects in the titania support stabilize the Au nanoparticles [46], and DFT studies also indicate that oxygen vacancies dictate the dispersion and shape of the Au clusters on titania [35].

In the work reported here, vapor-deposited Au clusters on $TiO_2$(110) exhibit activity for oxidation of methanol to formaldehyde, as studied by temperature programmed desorption experiments in ultrahigh vacuum. Investigations on these model systems provide valuable insight into understanding the mechanism of oxidation reactions on the Au–titania systems. Methanol is used as a probe molecule because the reaction of methanol on titania single-crystal surfaces, crystalline films and powders has been well studied [64–68]. In addition, the chemistry of methanol on bulk Au surfaces and other noble metals like Cu and Ag have been investigated in detail [69–76], given that Cu and Ag comprise the industrial catalysts used in oxidation of methanol to formaldehyde [69]. Furthermore, the partial oxidation of alcohols is a reaction of considerable industrial importance because these chemical processes are used in the production of commodity chemicals, as well as starting materials for many organic synthesis reactions [77]. Understanding the catalytic oxidation of methanol is also critical for the development of direct methanol fuel cells [78]. In the reaction of methanol on Au clusters on $TiO_2$ (Au/$TiO_2$), both Au and titania sites are necessary. Isotopic labeling experiments involving $CD_3OH$ and the incorporation of $^{18}O$ into the $TiO_2$ lattice illustrate that the role of the titania support is to initiate the reaction by facilitating O – H bond scission in methanol, and lattice oxygen is incorporated into water that desorbs from the surface. The role of the Au sites is to remove surface hydrogen as $H_2$, thus preventing recombination of methoxy and surface hydrogen and allowing methoxy to produce formaldehyde at higher temperatures. The dependence of formaldehyde yield on Au coverage suggests that the reaction occurs at Au–titania interfacial sites.

## 2. Experimental methods

Experiments were performed in two ultrahigh vacuum chambers with base pressures of $\leq 6\times10^{-11}$ Torr. Temperature programmed desorption (TPD) experiments were carried out in the first chamber, which was equipped with a shielded quadrupole mass spectrometer (Hiden HAL 301/3F), a cylindrical mirror analyzer for Auger electron spectroscopy (Omicron, CMA 150) and low energy electron diffraction options (Specs) [79–81]. STM and XPS experiments were conducted in the second chamber, which has a variable-temperature STM (Omicron, VT-25), a hemispherical analyzer for XPS experiments (Omicron, EA125), as well as a LEED/Auger system (Omicron, SPEC3) and a quadrupole mass spectrometer (Leybold Inficon Transpector 2) [81–84]. Both chambers have been previously described in greater detail [79–84].

The $TiO_2$ crystals (1 cm × 1 cm × 0.1 cm, Princeton Scientific Corporation) were mounted on a Ta backplate, which was heated by electron bombardment [80,85]. The temperatures were measured with either a type C or K thermocouple, which was spot welded to the backplate and calibrated with an infrared pyrometer [82]. The crystals were cleaned by several cycles of Ar ion sputtering (20 min, 1 kV, 2–4 μA current to the crystal) followed by annealing for 1–3 min at temperatures above 950 K. The cleanliness and order of the $TiO_2$(110)-(1 × 1) surfaces were confirmed using a combination of STM, LEED, AES and XPS.

In the first chamber, Au was deposited at room temperature at a rate of 0.1 ML/min from a pure Au pellet (Alfa Aesar, 99.9995%) housed inside a resistively heated W wire cage. In the second chamber, Au was deposited at room temperature using a commercial evaporator (Oxford Applied Research, EGC04) from a Au pellet in a Mo crucible; the sample was biased at +800 V during deposition to repel high energy Au ions. The Au deposition rates were established with an independently calibrated quartz crystal microbalance (Inficon) [84], and 1 ML of Au is defined with respect to the packing density of the Au(111) surface ($1.40\times10^{15}$ atoms/cm$^2$).

$CH_3OH$ (Sigma-Aldrich, 99.93%) and $CD_3OH$ (Cambridge Isotope Laboratories, 99.5%) were purified by several freeze–pump–thaw cycles before use. Oxygen ($O_2$, Matheson, 99.997%) and $^{18}O_2$ (Sigma Aldrich, 97%) were used as received. The surface was exposed to all adsorbate gases using a stainless steel directed dosing tube [83], which was positioned 2 mm from the face of the crystal, so that the local pressure at the surface was higher than the background chamber pressure and dosing onto the sample holder could be minimized. For the TPD experiments, the surface was exposed to methanol at 100 K and a pressure of $1.5\times10^{-11}$ Torr above the base pressure for 7 s, and this resulted in a saturation exposure, based on the desorption of methanol multilayers in the TPD experiments. For the XPS experiments, the surface was exposed to a saturation dose of methanol at room temperature (ΔP =

$4.5\times10^{-10}$ Torr, 45 s). Although the cracking pattern for methanol showed an 18 amu signal that was 3–7% of the 31 amu signal, we do not believe that water contamination was a serious issue because the methanol TPD experiments were not affected by variations in the 18:31 amu ratio for different methanol samples. Oxygen exposures were carried out at sample temperatures of 300 K and 800 K using a pressure increase of $1\times10^{-7}$ Torr for 5 min.

The experimental setup for the TPD experiments is described in more detail elsewhere [81]. Briefly, the crystal was heated with a linear temperature ramp of 2 K/s and was biased at −100 V to prevent damage from the electrons emitted by the mass spectrometer filament. Unless otherwise specified, nine masses were collected in a single experiment to optimize both the signal/noise ratio and the temperature resolution. For the wide mass scan experiments, as many as 40 mass channels were monitored in single experiment with lower temperature resolution in order to establish that there were no masses detected other than the ones corresponding to the identified products.

XPS experiments were conducted with an Al Kα anode, and the Ti(2p), O(1s) and Au(4f) regions were collected using acquisition parameters of: 0.2 s dwell time, 0.02 eV step size, and a 66° off normal detection angle. STM images were collected using electrochemically etched tungsten tips [84] at a +1.7 eV sample bias and 0.1 nA tunneling current. For both the XPS and STM studies, surfaces were annealed at a ramp rate of ~2 K/s and held at the desired temperature for 1 min.

## 3. Results

The chemical activity of methanol on the $TiO_2$(110) support surface is shown in Fig. 1a. In these experiments the surface is exposed to methanol at 100 K and then heated with a 2 K/s temperature ramp in front of the mass spectrometer. Although near stoichiometric $TiO_2$(110) surfaces are known to be inactive for methanol decomposition [67,68], the reduced $TiO_2$ surface studied here produces methyl radical (15 amu) as the major product at 640 K; the magnitude of this peak is known to increase as the surface becomes more reduced with additional sputter–anneal cycles. The desorption of methyl radicals in this temperature range (450 K–600 K) has also been observed for the decomposition of methoxy intermediates from: methanol reaction on oxidized Mo(110) [86]; dimethyl methylphosphonate reaction on $TiO_2$(110) [83,87]; and methyl adsorption on $Fe_2O_3$ [88]. $H_2$ desorption is detected at 280 K, and water is evolved in two features at 285 K and 480 K. A small amount of methane (16 amu) is produced in a broad peak extending from 400 to 700 K. The desorption of methanol itself (32 amu) occurs in a sharp peak at 140 K and in a second desorption feature at 290 K. The 140 K peak continues to grow in intensity as the methanol exposure is increased and is therefore assigned to the desorption of condensed methanol. The 290 K feature reaches its maximum intensity when the surface is saturated and is attributed to a methanol species bound directly to the surface. Note that the peaks at 140 K and 290 K in the 15 and 30 amu signals

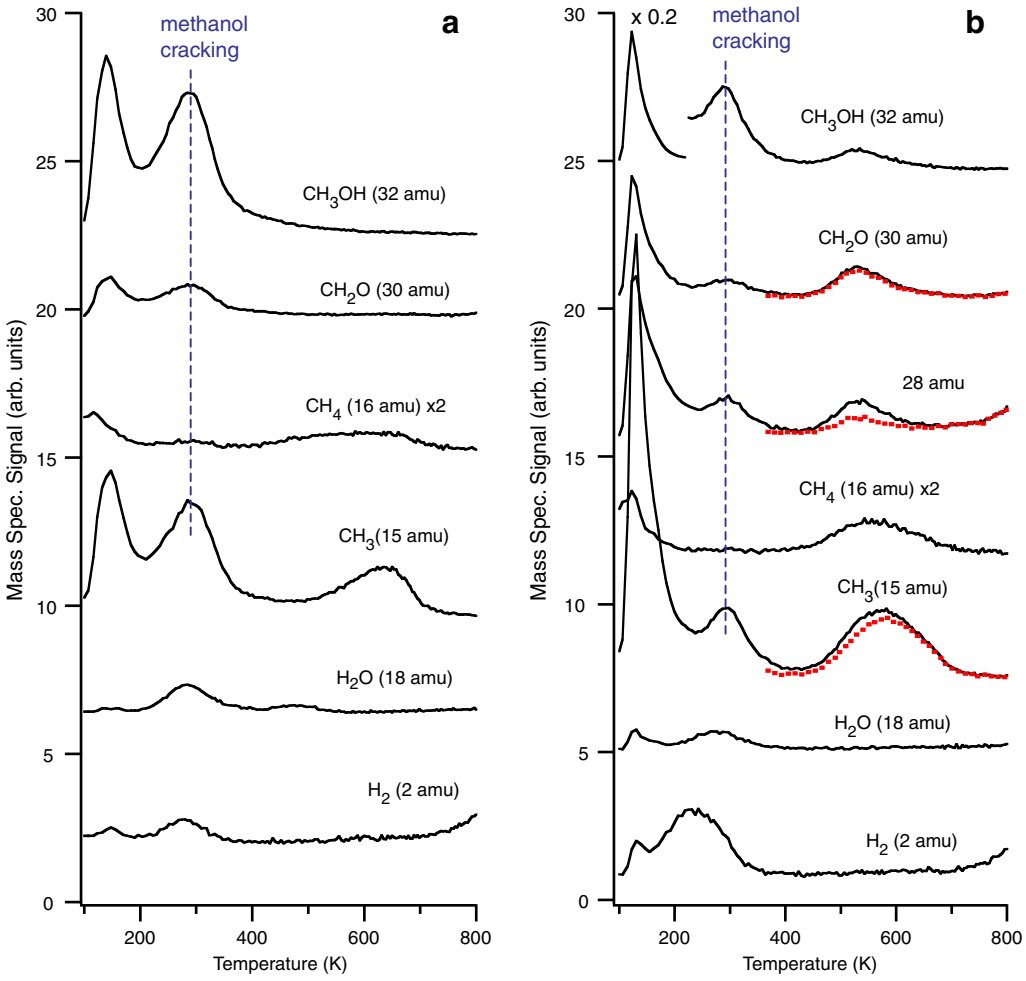


**Fig. 1.** Temperature programmed desorption data for methanol adsorbed at 100 K on: a) $TiO_2$(110) and b) 0.25 ML of Au on $TiO_2$(110). The dotted red lines are the signals after correcting for the cracking contributions of formaldehyde and methanol.

are ascribed to the fragmentation of methanol rather than the desorption of new products since the 15:30:32 ratio for methanol leaked into the chamber matches the respective ratios for the integrated desorption peaks. All masses from 1 to 110 amu were monitored in wide mass scan TPD experiments, and no masses other than those associated with cracking from the reported products are detected. Specifically, there is no signal at 28 amu from CO, 44 amu from $CO_2$, 30 amu from formaldehyde or 32 amu from methanol at high temperature.

The 0.25 ML Au clusters deposited on $TiO_2$(110) are active for methanol reaction (Fig. 1b) despite the fact that bulk Au surfaces are inert. A new product observed on the Au clusters is formaldehyde at 535 K, with methanol appearing at the same temperature. In addition, $H_2$ (2 amu) is evolved at 245 K while a less intense water feature (18 amu) is observed at 275 K. The surface sites that produce water at 480 K on clean $TiO_2$ are apparently passivated in the presence of the Au clusters. A peak from methyl radical desorption appears at 580 K, and the lower desorption temperature compared to that on $TiO_2$, as well as the larger peak area, indicates that methyl production on this surface is not solely from reaction on the $TiO_2$ and that methyl production is most likely related to Au–titania sites. A broad methane peak at 16 amu is also observed at 565 K. Methanol desorption occurs at 285 K, and the associated 15 and 30 amu signals are assigned to the cracking fragments of methanol rather than new product formation. No $CO_2$ (44 amu), formic acid (46 amu) or methyl formate (60 amu) products were observed in this reaction. Furthermore, all masses between 1 and 110 amu were monitored in wide mass scan TPD experiments, and no mass signals were observed other than those corresponding to the products already mentioned and the associated cracking fragments.

Product identification and analysis of the mass fragmentation patterns were carried out as follows. The 31:32 amu ratio (1.6) in the TPD experiment for the 535 K peak was consistent with the cracking ratio of pure methanol; the 31:32 ratios were calculated from peak heights rather than peak areas since the falling baseline for the 32 amu signal due to lower temperature methanol desorption prevents accurate integration of the methanol peaks. Identification of the 30 amu peak as formaldehyde is based on the 30:29 ratio (0.6) after correcting these masses for the cracking contribution of methanol. The ratios of 29 and 30 amu with 32 amu for methanol were established by leaking pure methanol into the chamber, and the 30:29 ratio for formaldehyde was taken from the NIST database [89].

The dotted traces shown for the 15, 28 and 30 amu peaks at 535 K in Fig. 1b are the signals after correcting for the contribution of methanol and formaldehyde in the 28 amu signal and methanol in the 15 and 30 amu signals. After correction, ~40% of the original intensity in the 28 amu peak still remains, and this suggests that CO is also produced from methanol reaction. The 28 amu signal was corrected in the following manner: 1) for methanol contribution, the 32 amu signal was multiplied by a factor of 0.27 and subtracted from the 28 amu signal since the 28:32 amu ratio is 0.27 in pure methanol; 2) for formaldehyde contribution, the 30 amu signal was multiplied by 0.41 and subtracted from the methanol-corrected 28 amu signal, based on the 28:30 amu ratio of 0.41 in the NIST database [89]. In the case of the methanol-corrected 30 amu signal, the 32 amu signal was multiplied by 0.16 and subtracted from the 30 amu signal, based on the 30:32 ratio for pure methanol; this correction has only a small effect on the 30 amu signal, which decreases by ~5%. The 32 amu signal was multiplied by 0.65 and subtracted from the 15 amu signal to generate the methanol-corrected 15 amu data shown in Fig. 1b. The methanol cracking accounted for 10% of the integrated 15 amu peak at 580 K.

The yields for the main products, formaldehyde and methyl, are shown in Fig. 2 as a function of Au coverage, and all yields are normalized to the values for reaction on 0.25 ML of Au. There is no formaldehyde production on clean $TiO_2$, and the formaldehyde yield remains near its maximum value between 0.25 and 1 ML (Fig. 2a). At higher Au coverages, formaldehyde production decreases sharply, dropping to 30% of the value at 0.25 ML at a Au coverage of 5 ML. Therefore,

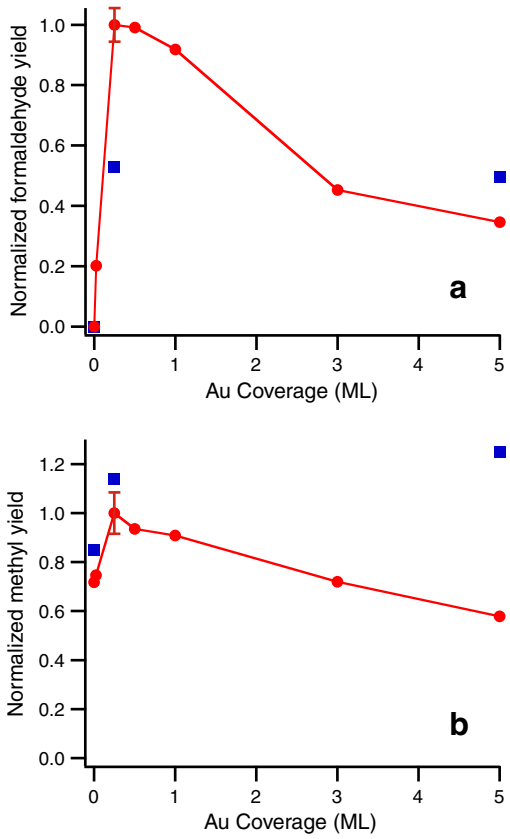


**Fig. 2.** A plot of normalized product yields from methanol reaction as a function of Au coverage for: a) formaldehyde (30 amu) and b) methyl (15 amu). The red circles represent experiments on unannealed Au clusters, and the blue squares are from reaction on Au clusters annealed to 800 K for 1 min. All values were normalized to the integrated signal for reaction on the unannealed 0.25 ML Au clusters. Yields were determined from the integrated peak intensities at 30 amu in the TPD experiments, and the 15 and 30 amu signals were corrected for cracking contributions from methanol. The error bars shown for the 0.25 ML coverage are the standard deviations from 4 experiments for the unannealed clusters and 2 experiments for the annealed clusters.

production of formaldehyde does not occur on pure Au sites since the yield decreases as the Au coverage is increased, and this suggests that the Au titania interfacial region may constitute the active sites. The methanol signal at 535 K also decreases with increasing Au coverage, but these values are harder to quantify due to the falling baseline for the 32 amu signal as a result of the large methanol desorption feature at 290 K. The blue squares in Fig. 2a represent the yields for the 0.25 ML and 5 ML Au clusters after annealing to 800 K for 5 min. After heating, the decrease in yield for the 0.25 ML clusters can be explained by loss of perimeter sites due to the sintering of the Au clusters. In contrast, the yield after heating the 5 ML clusters increases, presumably because sintering of this Au film exposes more of the Au–titania interface. Notably, the decrease in formaldehyde signal with increasing Au coverage cannot be explained solely by a loss of $TiO_2$ surface area because the annealed 0.25 ML Au clusters exhibit lower formaldehyde production despite the increase in $TiO_2$ surface area. The methyl yield shown in Fig. 2b indicates that the addition of small amounts of Au (0.25–1 ML) enhances methyl production compared to the $TiO_2$ surface itself, but increasing the Au coverage up to 5 ML drops the methyl yield slightly below the value for clean $TiO_2$. Thus, Au–titania interfacial sites may also contribute to methyl production. Furthermore, annealing the Au clusters to 800 K for 5 min increases methyl production by 14% on the 0.25 ML clusters and by more than a factor of 2 on the 5 ML clusters. Annealing the clean $TiO_2$ surface to the same temperature increased the methyl yield by 18%. The large increase in methyl yield for 5 ML

annealed Au clusters implies that heating enhances the interaction between Au and titania that promotes methyl formation.

STM images of the Au clusters confirm that the Au–titania interfacial sites decrease with increasing Au coverages (Fig. 3). The 0.25 ML Au clusters (Fig. 3a) have the smallest cluster sizes and therefore the greatest number of Au–titania interfacial sites. As the coverage is increased to 2 ML (Fig. 3b), larger clusters are formed as a result of coalescence, and the number of perimeter sites consequently decreases. At 5 ML (Fig. 3c), the cluster size continues to increase and the cluster coalescence is even more pronounced; here the surface begins to resemble a Au film rather than discrete clusters. The larger cluster sizes produced after heating the 0.25 ML clusters to 800 K decreases the number of interfacial sites (Fig. 3d). In contrast, annealing the 5 ML clusters to the same temperature increases the interfacial region because more of the titania surface is exposed as larger Au islands are formed (Fig. 3e). A more quantitative analysis of perimeter sites and formaldehyde yield is not possible because the diameters of the clusters measured by STM are known to be overestimated from tip convolution effects [84]. However, on a qualitative level, the STM images illustrate that the surfaces with the greatest number of Au–titania interfacial sites produce the highest formaldehyde yield from methanol reaction.

The role of surface oxidation in formaldehyde production is explored with oxidation treatments before and after Au deposition (Fig. 4), and in all cases, oxidation promotes formaldehyde production. The mass 30 amu signal in the TPD experiment for methanol on 0.25 ML Au on untreated $TiO_2$ is shown at the bottom of Fig. 4 for comparison. In all of the oxidation experiments, the surface is exposed to an $O_2$ pressure of $1\times10^{-7}$ Torr for 5 min at room temperature. The 29:30 amu ratio for the peak at 535 K was the same for reaction on all of the surfaces shown in Fig. 4, confirming that formaldehyde is produced in all cases. The peak at 290 K is from cracking of methanol, which desorbs at this temperature. For the 0.25 ML Au clusters treated with $O_2$ at 300 K and then exposed to methanol at 100 K, the formaldehyde yield increases by ~40%, and the onset for formaldehyde evolution decreases from 440 K to 405 K. Oxidation at a higher pressure ($5\times10^{-7}$ Torr) did not further increase the formaldehyde yield. It is also important to understand how oxidation changes the activity of the $TiO_2$ surface itself, which does not produce any formaldehyde in the absence of oxidation. On $TiO_2$ oxidized at 300 K, a formaldehyde peak appears at 645 K, which is 110 K higher than that observed on the Au clusters; this implies that the surface sites

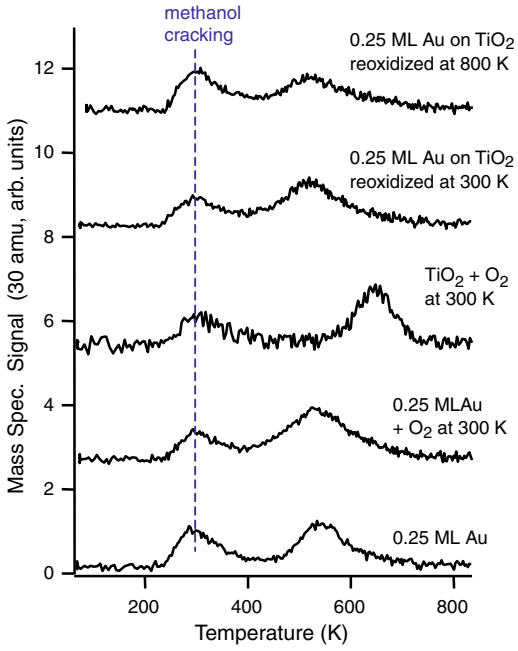


**Fig. 4.** Temperature programmed desorption data for formaldehyde production (30 amu) from methanol reaction on the following surfaces (bottom to top): 0.25 ML of Au on untreated $TiO_2$; 0.25 ML Au exposed to $O_2$ at 300 K; $TiO_2$ exposed to $O_2$ at 300 K; 0.25 ML of Au on $TiO_2$ exposed to $O_2$ at 300 K before Au deposition; and 0.25 ML of Au on $TiO_2$ exposed to $O_2$ at 300 K before Au deposition. All $O_2$ exposures were at a pressure of $1\times10^{-7}$ Torr for 5 min. The surfaces were initially exposed to a saturation dose of methanol at 100 K, and then flashed to 250 K in order to remove condensed methanol before the TPD experiment.

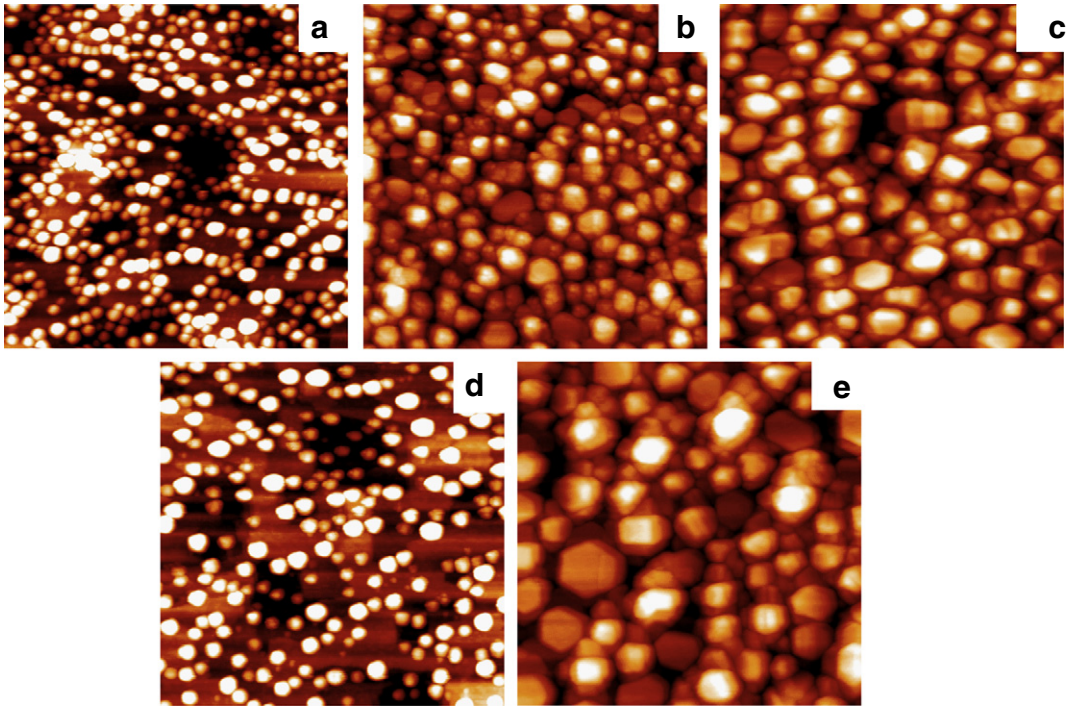


**Fig. 3.** Scanning tunneling microscopy images for Au clusters deposited on $TiO_2$ at room temperature for coverages of: a) 0.25 ML; b) 2 ML; c) 5 ML; d) 0.25 ML annealed at 800 K for 1 min; and e) 5 ML annealed at 800 K for 1 min. All images are 1000 Å × 1000 Å.

that give rise to formaldehyde on oxidized $TiO_2$ are different from the sites that produce formaldehyde on the 0.25 ML Au clusters. When 0.25 ML of Au is deposited on the reoxidized $TiO_2$, methanol reaction produces roughly the same amount of formaldehyde as on 0.25 ML of Au on untreated $TiO_2$, but the onset for formaldehyde production is still shifted to lower temperatures. Furthermore, when oxidation of $TiO_2$ is carried out with the same exposure at 800 K, the production of formaldehyde is ~90% of the value for 0.25 ML of Au on untreated $TiO_2$, and the onset of formaldehyde production still shifts to 410 K. Less oxygen is incorporated into the titania lattice for oxidation at 800 K compared to 300 K, based on the smaller contribution from the $Ti^{+3}$ peak in X-ray photoelectron spectroscopy experiments for oxidation at 300 K (data not shown). Formaldehyde is not observed at 645 K for the Au clusters on oxidized $TiO_2$, indicating that the presence of Au passivates the sites that produce the 645 K formaldehyde on oxidized $TiO_2$.

Isotopic labeling experiments with $^{18}O_2$ were carried out in order to understand the role of lattice oxygen in methanol reaction (Fig. 5). The sputtered/annealed $TiO_2$ surface was exposed to $^{18}O_2$ at a pressure of $1\times10^{-7}$ Torr for 5 min at room temperature before deposition of 0.25 ML of Au, followed by exposure to methanol at 100 K. The TPD experiment shows that $H_2^{18}O$ (20 amu) is produced at 270 K in addition to $H_2^{16}O$ (18 amu), demonstrating that lattice oxygen from titania is incorporated into the desorbing water. The evolution of methyl (15 amu), formaldehyde (30 amu), and methanol (32 amu) at 535 K are observed, as on the 0.25 ML Au clusters on unoxidized $TiO_2$. There is no evidence that $^{18}O$–methanol or $^{18}O$–formaldehyde are formed: no 35 or 36 amu signals are detected from $^{18}O$–methanol, and the 29:30 amu ratio is identical to that for reaction on 0.25 ML Au without oxidation. Furthermore, the $H_2$ peak at 245 K disappears, while the $H_2O$ signal increases for reaction on the 0.25 ML Au clusters deposited on oxidized versus unoxidized surfaces. Very little $H_2O$ is produced from 0.25 ML Au clusters on unoxidized $TiO_2$. In contrast, for the 0.25 ML Au clusters on oxidized $TiO_2$, the production of $H_2O$ accounts for all of the surface hydrogen, while no $H_2$ is evolved from reaction on oxidized $TiO_2$. Table 1 shows the product yields for methanol reaction on various surfaces and clearly illustrates that the selectively for $H_2$ and $H_2O$ at low temperature shifts toward $H_2O$ formation when there is excess oxygen on the surface. For reaction on Au clusters deposited on $TiO_2$ reoxidized at 800 K, 20 amu from $H_2^{18}O$ is still observed. This shows that the $^{18}O$ incorporated into $H_2^{18}O$ is not from oxygen adatoms produced when $^{18}O_2$ dissociates at oxygen vacancies since oxygen adatoms do not remain on the surface at 800 K. $H_2^{18}O$ accounts for ~60% of the total water production after 800 K oxidation compared to ~75% after 300 K oxidation. Furthermore, the magnitude of the 20 amu signal for 800 K oxidation is only 15% of the 20 amu signal for 300 K oxidation, and this implies that the majority of the water desorption on oxidized $TiO_2$ is from reaction of hydrogen with surface oxygen rather than lattice oxygen.

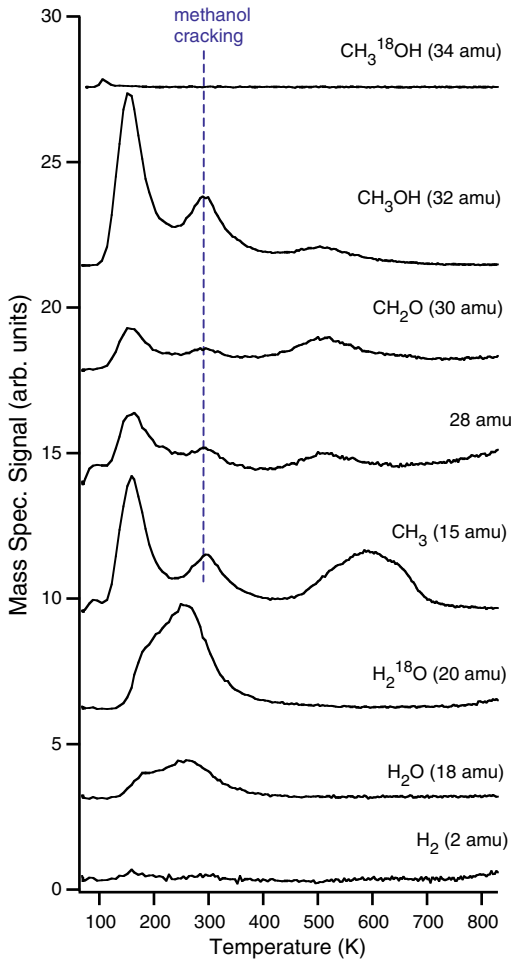


**Fig. 5.** Temperature programmed desorption data for a saturation exposure of methanol adsorbed at 100 K on 0.25 ML of Au on a $TiO_2$ surface that was exposed to $^{18}O_2$ ($1\times10^{-7}$ Torr, 5 min, 300 K) before Au deposition.

TPD experiments with $CD_3OH$ were also conducted to help elucidate the details of the reaction mechanism. On $TiO_2$, the data is consistent with O–H bond scission at low temperature, followed by C–O bond breaking to produce $CD_3$ at higher temperature. $CD_3OH$ reaction produces $CD_3$ (18 amu) as the main product along with small amounts of $H_2$ (2 amu) at 275 K (Fig. 6). Potential water (18 amu) desorption at low temperature cannot be deconvoluted from the large methanol cracking feature at 290 K. The 19 amu signal is assigned to $CD_3H$ since it has the same peak shape and temperature as $CH_4$ (16 amu) produced from $CH_3OH$ reaction. Given that hydrogen does not remain on the surface at this temperature, the hydrogen that combines with $CD_3$ is likely to be from the chamber background. No $D_2O$ (20 amu) desorption is observed, which indicates that C–D bond scission does not occur below the usual temperature for water desorption. At higher temperatures, $H_2$ and HD (3 amu) signals are not detected although trace amounts of $D_2$ (4 amu) desorb at 630 K.

For $CD_3OH$ reaction on 0.25 ML Au clusters (Fig. 7), only H-containing products evolve at temperatures below 350 K, while only deuterium-containing products evolve at high temperatures, demonstrating that initial reaction occurs via O–H bond scission at low temperature. $H_2O$ desorption at 275 K may also occur but cannot be detected due to the fragmentation of desorbing $CD_3OH$ at 18 amu. No $D_2O$ or $D_2$ are detected at temperatures below 400 K. This implies that reaction initially occurs via O–H rather than C–D bond scission, and methoxy is the likely intermediate. The absence of any H-containing products above 400 K is also consistent with methoxy formation at low temperature. The 18 amu signal at 560 K is assigned primarily to $CD_3$ rather than $H_2O$ because the 18 amu signal has the same peak shape and intensity as the 15 amu signal from $CH_3$ in $CH_3OH$ reaction.

The only formaldehyde species that is produced is $d_2$-formaldehyde ($CD_2O$), which arises from selective C–D bond scission in the methyl group. The 32:30 amu ratio is consistent with the corresponding 30:29 amu ratio observed for $d_0$-formaldehyde from $CH_3OH$ reaction, confirming product identity. Above 400 K, the absence of $CD_3OH$ desorption at 35 amu demonstrates that all of the hydroxyl hydrogens have desorbed from the surface as $H_2O$ or $H_2$. The only methanol species detected is $CD_3OD$ (36 amu), which desorbs concomitantly with formaldehyde. After removing the contribution from the cracking of methanol and formaldehyde from the 28 amu signal, the remaining signal is attributed to CO formation and accounts for ~40% of the uncorrected signal, as in the case of $CH_3OH$ reaction. The 19 and 20 amu signals are assigned to $CD_3H$ and $CD_4$, respectively, rather than $D_2O$. The combined 19 and 20 amu signal is identical in peak shape and intensity to the 16 amu signal from $CH_4$ in $CH_3OH$ reaction. Thus, the $CD_4$ is attributed to combination of $CD_3$ with surface D atoms released by C–D bond

**Table 1**
Product yields for methanol reaction on 0.25 ML Au clusters on $TiO_2$ and on $TiO_2$ itself after various oxidation treatments with $^{18}O_2$. All $^{18}O$–oxygen exposures were carried at $1\times10^{-7}$ Torr for 5 min. Integrated intensities are normalized to that of methanol reaction on 0.25 ML Au. Methanol intensities are from peak heights rather than integrated areas to avoid contribution from the falling baseline from methanol desorption at lower temperatures. The formaldehyde yields were corrected for the cracking contributions of methanol.

| | $H_2$ (2 amu) | Methyl (15 amu) | $H_2O$ (18 + 20 amu) | Formaldehyde (30 amu) at ~535 K | Methanol (32 amu) at ~535 K |
|---|---|---|---|---|---|
| $TiO_2$ untreated | 0.12 | 0.75 | 3.32 | 0 | 0 |
| $TiO_2$ exposed to $^{18}O_2$ at 300 K | 0 | 2.00 | 15.73 | 0 | 0 |
| 0.25 ML Au deposited on $TiO_2$ | 1.00 | 1.00 | 1.00 | 1.00 | 1.00 |
| 0.25 ML Au exposed to $^{18}O_2$ at 300 K | 0 | 1.03 | 14.56 | 1.52 | 1.24 |
| 0.25 ML Au deposited on $TiO_2$ exposed to $^{18}O_2$ at 300 K | 0 | 0.67 | 13.91 | 1.27 | 1.18 |
| 0.25 ML Au deposited on $TiO_2$ exposed to $^{18}O_2$ at 800 K | 0.83 | 0.82 | 2.79 | 0.80 | 0.78 |

breaking in $d_3$-methoxy, while the $CD_3H$ is attributed to the addition of H from the background to $CD_3$.

The production of $CD_3OD$ at 540 K is significantly diminished compared to methanol formed from the reaction of $CH_3OH$. For the deuterated case, the methanol:formaldehyde peak area ratio is $0.47\pm0.07$ (36:32 amu), whereas the corresponding ratio of $0.71\pm0.03$ (32:30 amu) is significantly higher in the nondeuterated case; the error bars are the standard deviations from 3 and 5 identical experiments with $CD_3OH$ and $CH_3OH$, respectively. The deuterium atoms released by C – D bond scission during formaldehyde production form $D_2$ (4 amu) at a peak temperature of 610 K. In contrast, very little $H_2$ was observed at this temperature from the reaction of $CH_3OH$, suggesting that most of the surface hydrogens combine with the methoxy intermediate to form methanol. The integrated area of the 610 K $H_2$ peak from $CH_3OH$ reaction was only ~10% of that for the $D_2$ peak from $CD_3OH$ reaction. There is also a 10–13 K shift to higher temperature in the production of $CD_3OD$ from $d_3$-methanol compared to $CH_3OH$ from $d_0$-methanol. Given that the temperature resolution for this experiment was 3 K, the observed shift is small but outside the range of experimental error. In the reaction of $CD_3OH$, the deuterium atoms liberated from C – D scission in methoxy can form $D_2$ rather than diffusing to another neighboring methoxy to recombine and produce methanol; the diminished methanol evolution

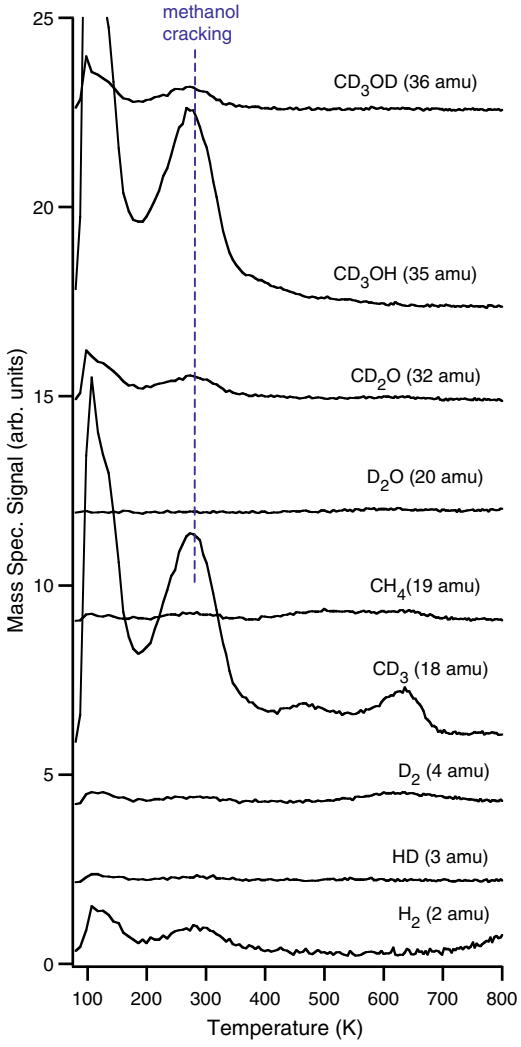


**Fig. 6.** Temperature programmed desorption data for a saturation exposure of $CD_3OH$ adsorbed at 100 K on $TiO_2$.

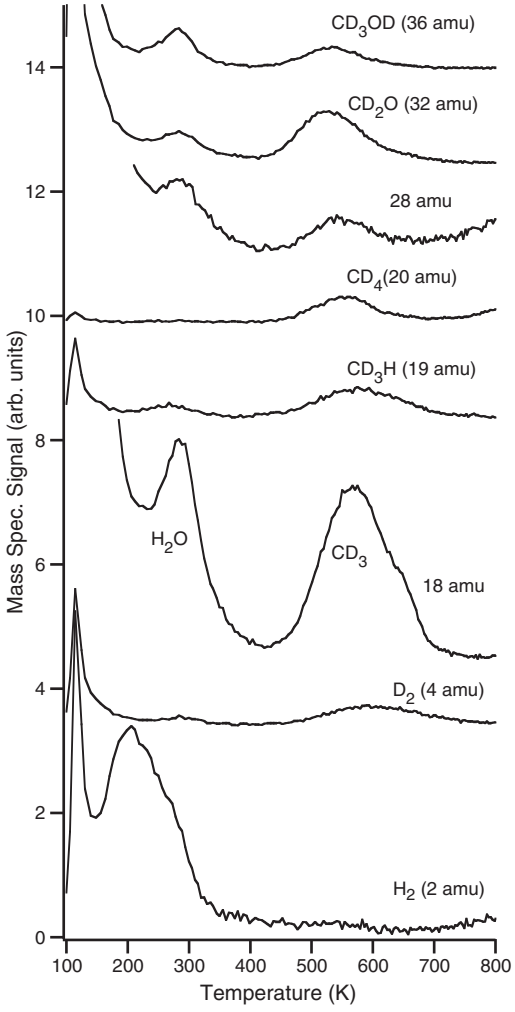


**Fig. 7.** Temperature programmed desorption data for a saturation exposure of $CD_3OH$ adsorbed at 100 K on 0.25 ML of Au on $TiO_2$.

and high desorption temperature are attributed to slower diffusion of deuterium atoms on the surface compared to hydrogen atoms.

C – D bond scission is *not* the rate limiting step in formaldehyde evolution on the Au clusters because no kinetic isotope effect is observed for the desorption of formaldehyde in $CD_3OH$ reaction. If C – H(D) bond breaking is the rate-limiting step in formaldehyde production, the formaldehyde desorption peak should shift to higher temperature for the reaction of $CD_3OH$ compared to undeuterated methanol, but no such shift is observed. This behavior is in contrast with what is reported as the mechanism for aldehyde or ketone production from alcohol reaction on many transition metal surfaces [76,90–92]. For example, on O – Cu(111) [76], a significant deuterium kinetic isotope effect is observed for $CD_3OH$: the desorption temperature for $d_2$-formaldehyde is shifted to higher temperatures by $28 \pm 2$ K compared to $d_0$-formaldehyde desorption from $CH_3OH$ reaction. This corresponds to an activation energy of 24.5 kcal/mol for $CH_3OH$ compared to 26.2 kcal/mol for $CD_3OH$, assuming $\nu = 10^{13}\ s^{-1}$ at a heating rate of 2 K/s. Since our experimental heating rate is identical, we would expect a comparable shift in desorption temperature, but the temperature for formaldehyde evolution on the Au clusters is not shifted at all.

X-ray photoelectron spectroscopy data for the Ti(2p) region were collected after heating methanol to various temperatures on $TiO_2$ and $Au/TiO_2$ in order to study changes in the oxidation state of titania (Fig. 8). Experiments were conducted at grazing angle detection to enhance the surface sensitivity, and all spectra were normalized to the intensity of the Ti($2p_{3/2}$) peak for clean $TiO_2$(110) so that small changes in peak shape could be more readily observed. When the $TiO_2$ surface itself is exposed to a saturation dose of methanol at room temperature and heated to 450 K and 700 K, there is no change in the Ti(2p) binding energy or peak shape (Fig. 8a), indicating that the oxidation state of titania is unchanged in methanol reaction. In the case of 0.25 ML of Au on $TiO_2$, methanol exposure at room temperature causes a slight decrease of the low binding energy shoulder around 456.5 eV (Fig. 8b). This shoulder is attributed to the contribution of reduced titania, mostly $Ti^{+3}$, and the disappearance of the shoulder indicates that the surface is slightly oxidized. Furthermore, heating to 450 K and then 750 K reduces the surface back to its original oxidation state prior to methanol exposure. Thus, it appears that in the presence of Au clusters, methanol is able to oxidize the titania surface, indicating that methanol adsorbs on $TiO_2$ rather than Au. For methanol on clean $TiO_2$, the $Ti^{+3}$ species does not appear to be oxidized at 300 K because water desorption removes oxygen from the surface. In contrast, on the Au clusters, the hydroxyl hydrogen from methanol desorbs primarily as $H_2$ rather than water, and oxygen from methoxy remains on the surface.

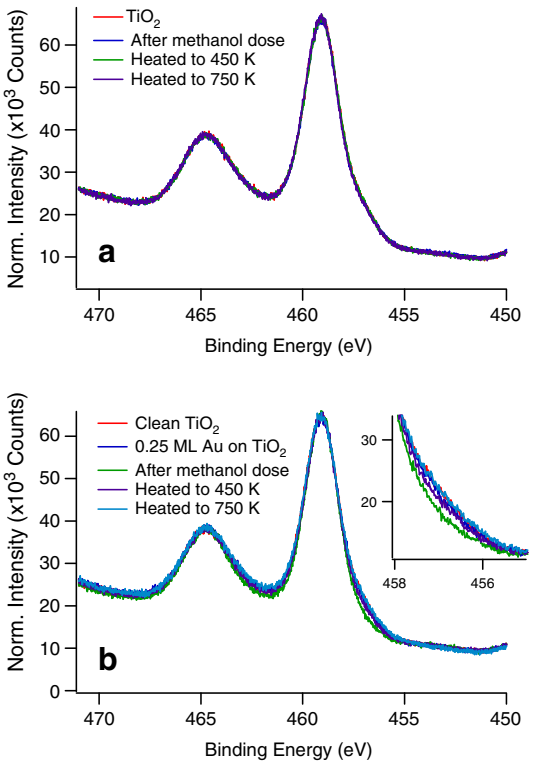


**Fig. 8.** X-ray photoelectron spectroscopy data for the Ti(2p) region for a saturation exposure of methanol on: a) $TiO_2$ and b) 0.25 ML of Au on $TiO_2$; after room temperature exposure and heating to various temperatures. Experiments were carried out at detection angle of 66° off normal to enhance surface sensitivity. Spectral intensities are normalized to the value for clean $TiO_2$ at room temperature so that small differences in peak shape can be observed. The surfaces were exposed to methanol at a pressure of $3 \times 10^{-10}$ Torr for 45 s at room temperature.

## 4. Discussion

Au clusters on $TiO_2$(110) exhibit activity for methanol oxidation to formaldehyde despite the fact that bulk Au surfaces [75,93] and the vacuum-annealed titania support are both inactive for this reaction. Formaldehyde is evolved as a major product at 535 K, with methanol desorption at the same temperature. The other desorption products from methanol reaction on the Au clusters are methyl radical at 560 K, water at 275 K and $H_2$ at 245 K. Isotopic labeling studies show that the key step in the methanol reaction is O – H bond scission, which is facilitated by the titania support. The role of oxygen from titania is to abstract a hydroxyl hydrogen in order to form the active methoxy species, and lattice oxygen is incorporated into the water that desorbs from the surface below 350 K. Upon further heating, methoxy undergoes selective C – H bond scission to produce formaldehyde, and the resulting hydrogen atoms recombine with methoxy to form methanol at the same temperature. XPS data indicate that in the presence of Au clusters, methanol oxidizes the titania surface. Since methanol oxidation does not occur on $TiO_2$ alone, this result demonstrates not only that methanol adsorbs on $TiO_2$ rather than the Au clusters, but also that the Au clusters play a significant role in methanol reaction. A proposed reaction mechanism is shown in Fig. 9.

The Au clusters facilitate further reaction in the methoxy intermediate by providing sites on which the removal of surface hydrogen as $H_2$ occurs. The $TiO_2$ surface itself has no activity for the conversion of methanol to formaldehyde despite the fact that the O – H bond scission readily occurs on this surface, as shown in this work as well as in numerous studies of methanol [64–66] and other alcohols [94–96] on titania single crystals, films and powders. While O – H bond breaking to form methoxy is facile on titania, recombination of methoxy and surface hydrogen results in desorption of methanol rather than further reaction. However, in the presence of Au clusters, the removal of surface hydrogen as $H_2$ is facilitated. This prevents methoxy from recombining with surface hydrogen, which results in the desorption of methanol rather than further reaction of methoxy.

Given that O – H bond scission in methanol occurs at $TiO_2$ sites and that the hydroxyl hydrogens recombine to form $H_2$ at Au sites, it is likely that the initial dissociation of methanol occurs at or near the Au–titania interface. The probability that a hydrogen atom will encounter a methoxy on $TiO_2$ and recombine to methanol must be lower than the probability of encountering another hydrogen atom to form $H_2$ on Au. Thus, methanol dissociation must occur at or near a Au cluster. Furthermore, this proposed activity at interfacial Au–titania sites is supported by the observed decrease in formaldehyde yield with increasing Au coverage, coupled with the STM images that show fewer Au–titania perimeter sites at higher Au coverages. Moreover, recent DFT studies of methanol on $Au_{13}$ on $TiO_2$(110) demonstrate that the preferred binding site for methoxy is at the Au–titania interface [97], and experimental evidence for reaction at the Au–titania interface has also been recently reported for CO oxidation on Au clusters on $TiO_2$ [63].

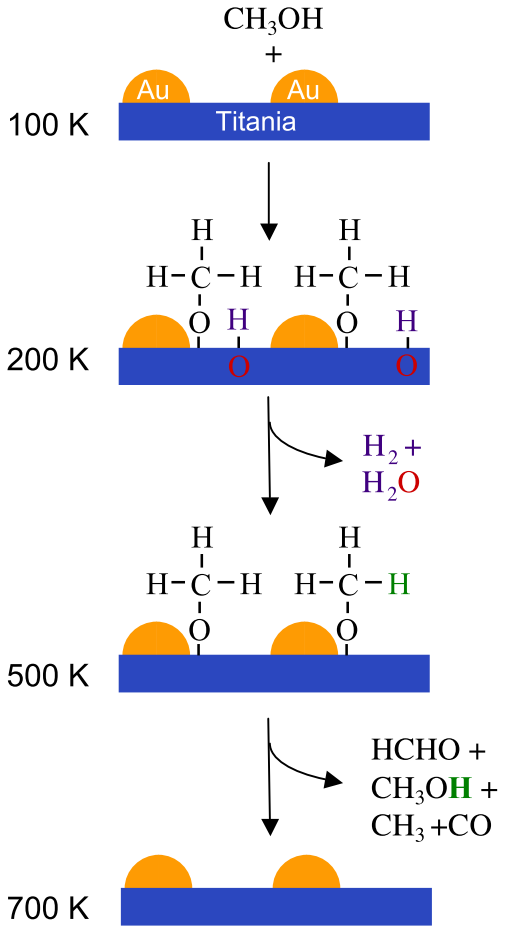


**Fig. 9.** A proposed scheme for methanol reaction on 0.25 ML Au clusters on $TiO_2$(110).

Similarly, it appears that methyl radical production occurs at a Au-modified $TiO_2$ site. On both $TiO_2$ and Au/$TiO_2$, the evolution of methyl radicals is observed between 500 and 700 K. On $TiO_2$, the adsorption of methoxy at oxygen vacancy defects results in C–O bond scission that produces gaseous methyl radicals and leaves oxygen behind on the surface. However, on the Au clusters, the peak temperature for methyl production is shifted to lower temperature by 80 K, and the methyl yield is higher on the Au clusters compared to that on clean $TiO_2$. Furthermore, it is likely that this reaction is also associated with active sites at the perimeter of the clusters, given that in the Au low coverage regime, the methyl yield initially increases with increasing Au deposition, but methyl production then decreases with increasing coverage as Au–titania interfacial sites are lost due to the coalescence of the Au clusters.

Oxidized $TiO_2$ exhibits activity similar to that of the Au clusters on $TiO_2$ because in both cases, formaldehyde is a major product and is accompanied by methanol desorption at the same temperature. Furthermore, in both cases, the modified titania surface provides a mechanism by which hydrogen from O–H bond scission can be removed from the surface to avoid recombination with methoxy. Excess oxygen on $TiO_2$ prevents reformation of methanol by removing surface hydrogen through the desorption of water below 400 K and leaving methoxy on the surface to form formaldehyde via subsequent C–H bond scission. The fact that the desorption temperature for formaldehyde is higher on oxidized $TiO_2$ (~600 K) compared to that on the Au clusters (~535 K) implies that the active site on titania is modified by Au, which promotes C–H bond scission in methoxy at lower temperatures. The increased formaldehyde and water production observed from methanol reaction for oxidized $TiO_2$, as well as for $TiO_2$ oxidized either before or after Au deposition, indicates that surface oxygen enhances O–H bond scission.

The high activity of the Au clusters on $TiO_2$ for methanol reaction is not attributed to undercoordinated Au atoms in the clusters, as has been suggested for CO oxidation on Au/$TiO_2$ [30,31,34–40]. TPD and XPS experiments clearly show that methanol adsorption occurs on the $TiO_2$ surface. Furthermore, when the 5 ML Au clusters were annealed to 800 K to increase cluster size, the formaldehyde yield *increased* with respect to unannealed clusters. Since smaller clusters have a greater number of undercoordinated Au atoms, the lower formaldehyde yield on the smaller clusters indicates that the undercoordinated Au atoms are not responsible for formaldehyde production. However, it is possible that the undercoordinated Au atoms on the cluster surfaces have some contribution to activity. For example, these undercoordinated Au atoms may enhance the activity of the Au clusters by: stabilizing the adsorption of methanol and methoxy at interfacial sites; promoting O–H bond scission in methanol; and promoting C–H bond scission in methoxy to produce formaldehyde. The production of a small amount of CO from methanol reaction on the Au clusters could be related to the high activity of undercoodinated Au atoms for nonselective C–H bond scission, which is not observed for methoxy on Au(111) surfaces [93].

The proposed mechanism for methanol reaction on Au/$TiO_2$ has also been observed for methanol reaction on a number of other noble metal surfaces, where O–H bond scission is followed by C–H bond cleavage in the methoxy intermediate to yield formaldehyde. For example, formaldehyde production via C–H bond scission in the methoxy intermediate is a reaction that is also observed on oxygen-covered noble metal surfaces like Ag [71,73] and Cu [69,70,72,76], and similar reaction processes are reported on oxygen-covered Au [74,75]. On both bulk metal surfaces and Au clusters, a crucial step in methanol reaction is dissociation of the O–H bond. While this process is promoted by the titania support for the Au clusters, atomic oxygen facilitates O–H bond scission on the noble metal surfaces, including Cu(110) [69,70], and Ag(111) [71]; in fact, O–H bond scission does not occur in the absence of surface oxygen on Cu(111) [72], Ag(110) [73], Au(111) [74], and Au(110) [75]. As on the $TiO_2$-supported Au clusters, formaldehyde and methanol desorb simultaneously with identical peak shapes on O–Cu(110) [69,70,76], O–Cu(111) [72] and O–Ag(111) [71]. However, formaldehyde and methanol desorption occurs at lower temperatures on the noble metal surfaces (290 K–450 K [69,71,76] vs. 535 K), implying that methoxy has greater thermal stability on the Au/$TiO_2$ surface than on the oxygen-covered noble metals.

It is unlikely that methanol reaction occurs on pure Au sites or oxygen-covered Au sites created by spillover of oxygen from the $TiO_2$ support because the activity of methoxy on the $TiO_2$-supported Au clusters is different from that on bulk Au surfaces as well as oxygen-modified Au surfaces. Au(111) [93] and (110) [75] are inactive for methanol reaction, but reaction occurs on O-covered Au surfaces, where the role of surface oxygen is to form the reactive methoxy intermediate by inducing O–H bond scission [97]; atomic oxygen is deposited via the decomposition of ozone on Au(111) [93,98], while $O_2$ dissociates on Au(110) to form an oxygen overlayer [75]. In addition to undergoing C–H bond scission to produce gaseous formaldehyde, products such as methyl formate and formic acid as well as $CO_2$ are evolved on O–Au(111) [93], but only methyl formate and $CO_2$ are produced on O–Au(110) [75]. Methyl formate is formed from the reaction of surface formaldehyde with methoxy, while formic acid and $CO_2$ arise from a formate intermediate. The absence of products like formic acid and $CO_2$ on the Au clusters is attributed to the lack of oxygen present on the cluster surfaces. Furthermore, the absence of methyl formate production on the Au clusters may indicate that methoxy and formaldehyde are not as mobile on the Au clusters as they are on bulk Au surfaces, and this would be consistent with a methoxy intermediate strongly bound to both Au and titania at an interfacial site [97].

The activity of methanol on $TiO_2$(110) observed in this work is very similar to studies reported previously [67,68]. The main difference is that our $TiO_2$ surface produces methyl radicals at 600 K from methanol reaction, whereas methyl radicals are not observed on

other near-stoichiometric $TiO_2$(110) surfaces [67,68]; notably, the {011}-facetted $TiO_2$(001) surfaces are more active than $TiO_2$(110), evolving methane and formaldehyde from methanol reaction [64]. Methyl radical production is attributed to reaction at oxygen vacancy defects, which promote C – O bond scission in methoxy in order to heal the oxygen vacancies. This type of mechanism was also proposed for the reaction of methanol on $TiO_2$ surfaces where oxygen vacancies were intentionally introduced by electron bombardment [68]. On these defective surfaces, C – O bond scission in methoxy was observed although the desorbing product was methane rather than methyl as in our experiments, and it was suggested that hydrogen from the background could contribute to methane formation following C – O bond scission in methoxy [68]. Notably, the promotion of C – O bond scission at oxygen vacancy defects has been observed for ethanol reaction on $TiO_2$(110) [94], as well as the reaction of methanol [64] and other aliphatic alcohols on {011}-facetted $TiO_2$(001) [64,95]. Given that our surfaces were heated to high temperatures (950–1000 K) in order to prepare a flat surface for STM studies, our crystal is more reduced than crystals that were heated only to 850 K [67] or reoxidized after sputtering [68]; this could explain the higher activity for methanol reaction on $TiO_2$(110) observed in our experiments.

## 5. Conclusions

The 0.25 ML Au clusters on $TiO_2$ exhibit unusual activity for the oxidation of methanol to formaldehyde, and this is attributed to a combination of activity at $TiO_2$ and Au sites. A key step in methanol reaction on Au/$TiO_2$ is O – H bond scission, which occurs on the titania support. Isotopic labeling studies in which the titania surface is oxidized with $^{18}O_2$ before or after Au deposition demonstrate that oxygen from titania participates in the reaction via the formation of $H_2^{18}O$, which desorbs at 250 K. XPS studies of methanol reaction on the Au/$TiO_2$ surface show that methanol adsorbs on $TiO_2$ since titania is oxidized by methanol in the presence of the Au clusters. The Au sites facilitate low temperature desorption of hydrogen from the surface as $H_2$, thus preventing recombination of surface hydrogen and methoxy and allowing methoxy to undergo C – H bond scission to produce formaldehyde. The desorption temperature for formaldehyde on Au/$TiO_2$ is lower than that on oxidized $TiO_2$, suggesting that reaction occurs at a Au-modified titania site. Similarly, methyl radical production may occur at Au-modified titania sites; although methyl formation is characteristic of reaction on titania rather than Au, the presence of Au shifts the methyl desorption to lower temperature and increases the yield. Furthermore, it is likely that reaction occurs at or near the Au–titania interfacial sites because the surface hydrogen atoms must be able to diffuse to the Au clusters and recombine as $H_2$ before they encounter a surface methoxy to form methanol. The formaldehyde yields as a function of Au coverage and the corresponding STM images are also consistent with formaldehyde production at the interfacial sites, given that the formaldehyde yield decreases with the number of sites at the perimeter of the Au clusters.

## Acknowledgments

We gratefully acknowledge financial support from the National Science Foundation (CHE 0845788) and the Department of Energy, Basic Energy Sciences (DE-FG02-07ER15842).

## References

[1] M. Haruta, T. Kobayashi, H. Sano, N. Yamada, Chem. Lett. (1987) 405.
[2] Y. Iizuka, T. Tode, T. Takao, K. Yatsu, T. Takeuchi, S. Tsubota, M. Haruta, J. Catal. 187 (1999) 50.
[3] M. Haruta, Catal. Today 36 (1997) 153.
[4] M. Haruta, S. Tsubota, T. Kobayashi, H. Kageyama, M.J. Genet, B. Delmon, J. Catal. 144 (1993) 175.
[5] G.R. Bamwenda, S. Tsubota, T. Nakamura, M. Haruta, Catal. Lett. 44 (1997) 83.
[6] M. Haruta, Cattech 6 (2002) 102.
[7] M. Haruta, Chem. Rec. 3 (2003) 75.
[8] M. Haruta, M. Date, Appl. Catal. A 222 (2001) 427.
[9] M. Haruta, N. Yamada, T. Kobayashi, S. Iijima, J. Catal. 115 (1989) 301.
[10] R. Meyer, C. Lemire, S.K. Shaikhutdinov, H. Freund, Gold Bull. 37 (2004) 72.
[11] T. Hayashi, K. Tanaka, M. Haruta, J. Catal. 178 (1998) 566.
[12] A.K. Sinha, S. Seelan, S. Tsubota, M. Haruta, Top. Catal. 29 (2004) 95.
[13] S.J. Ainsworth, Chem. Eng. News 70 (1992) 9.
[14] M.C. Kung, R.J. Davis, H.H. Kung, J. Phys. Chem. C 111 (2007) 11767.
[15] H.H. Kung, M.C. Kung, C.K. Costello, J. Catal. 216 (2003) 425.
[16] E. Antolini, Mater. Chem. Phys. 78 (2003) 563.
[17] B.D. McNicol, D.A.J. Rand, K.R. Williams, J. Power. Sources 83 (1999) 15.
[18] P. Waszczuk, G.Q. Lu, A. Wieckowski, C. Lu, C. Rice, R.I. Masel, Electrochim. Acta 47 (2002) 3637.
[19] Y.J. Mergler, J. Hoebink, B.E. Nieuwenhuys, J. Catal. 167 (1997) 305.
[20] C.T. Campbell, Science 306 (2004) 234.
[21] M. Chen, Y. Cai, Z. Yan, D.W. Goodman, J. Am. Chem. Soc. 128 (2006) 6341.
[22] M. Valden, X. Lai, D.W. Goodman, Science 281 (1998) 1647.
[23] C.C. Chusuei, X. Lai, K. Luo, D.W. Goodman, Top. Catal. 14 (2001) 71.
[24] D.W. Goodman, J. Phys. Chem. 100 (1996) 13090.
[25] J.D. Grunwaldt, A. Baiker, J. Phys. Chem. B 103 (1999) 1002.
[26] T. Fujitani, I. Nakamura, T. Akita, M. Okumura, M. Haruta, Angew. Chem. Int. Ed. 48 (2009) 9515.
[27] G. Bond, Gold Bull. 43 (2010) 88.
[28] C. Lemire, R. Meyer, S. Shaikhutdinov, H.J. Freund, Angew. Chem. Int. Ed. 43 (2004) 118.
[29] D.C. Meier, D.W. Goodman, J. Am. Chem. Soc. 126 (2004) 1892.
[30] N. Lopez, J.K. Norskov, J. Am. Chem. Soc. 124 (2002) 11262.
[31] M. Mavrikakis, P. Stoltze, J.K. Norskov, Catal. Lett. 64 (2000) 101.
[32] J. Guzman, B.C. Gates, J. Am. Chem. Soc. 126 (2004) 2672.
[33] J. Guzman, B.C. Gates, Angew. Chem. Int. Ed. 42 (2003) 690.
[34] N. Lopez, T.V.W. Janssens, B.S. Clausen, Y. Xu, M. Mavrikakis, T. Bligaard, J.K. Norskov, J. Catal. 223 (2004) 232.
[35] N. Lopez, J.K. Norskov, T.V.W. Janssens, A. Carlsson, A. Puig-Molina, B.S. Clausen, J.D. Grunwaldt, J. Catal. 225 (2004) 86.
[36] B. Hvolbaek, T.V.W. Janssens, B.S. Clausen, H. Falsig, C.H. Christensen, J.K. Norskov, Nano Today 2 (2007) 14.
[37] T.V.W. Janssens, B.S. Clausen, B. Hvolbaek, H. Falsig, C.H. Christensen, T. Bligaard, J.K. Norskov, Top. Catal. 44 (2007) 15.
[38] I.N. Remediakis, N. Lopez, J.K. Norskov, Angew. Chem. Int. Ed. 44 (2005) 1824.
[39] N. Lopez, J.K. Norskov, J. Am. Chem. Soc. 124 (2002) 11262.
[40] N. Lopez, J.K. Norskov, Surf. Sci. 515 (2002) 175.
[41] I.N. Remediakis, N. Lopez, J.K. Norskov, Appl. Catal. A 291 (2005) 13.
[42] S.H. Overbury, V. Schwartz, D.R. Mullins, W.F. Yan, S. Dai, J. Catal. 241 (2006) 56.
[43] J. Szoko, A. Berko, Vacuum 71 (2003) 193.
[44] T.V.W. Janssens, A. Carlsson, A. Puig-Molina, B.S. Clausen, J. Catal. 240 (2006) 108.
[45] M.S. Chen, D.W. Goodman, Catal. Today 111 (2006) 22.
[46] M.S. Chen, D.W. Goodman, Chem. Soc. Rev. 37 (2008) 1860.
[47] M.S. Chen, D.W. Goodman, Science 306 (2004) 252.
[48] A.A. Herzing, C.J. Kiely, A.F. Carley, P. Landon, G.J. Hutchings, Science 321 (2008) 1331.
[49] Y. Liu, C.J. Jia, J. Yamasaki, O. Terasaki, F. Schuth, Angew. Chem. Int. Ed. 49 (2010) 5771.
[50] M.M. Schubert, S. Hackenberg, A.C. van Veen, M. Muhler, V. Plzak, R.J. Behm, J. Catal. 197 (2001) 113.
[51] S.H. Overbury, L. Ortiz-Soto, H.G. Zhu, B. Lee, M.D. Amiridis, S. Dai, Catal. Lett. 95 (2004) 99.
[52] G.C. Bond, D.T. Thompson, Catal. Rev. Sci. Eng. 41 (1999) 319.
[53] S.D. Lin, M. Bollinger, M.A. Vannice, Catal. Lett. 17 (1993) 245.
[54] M.A. Bollinger, M.A. Vannice, Appl. Catal. B 8 (1996) 417.
[55] L.M. Molina, B. Hammer, Appl. Catal. A 291 (2005) 21.
[56] J.R. Monnier, Appl. Catal. A 221 (2001) 73.
[57] M. McCoy, Chem. Eng. News 79 (2001) 19.
[58] S. Lin, M.A. Vannice, Catal. Lett. 10 (1991) 47.
[59] J.A. Rodriguez, S. Ma, P. Liu, J. Hrbek, J. Evans, M. Perez, Science 318 (2007) 1757.
[60] S. Tsubota, T. Nakamura, K. Tanaka, M. Haruta, Catal. Lett. 56 (1998) 131.
[61] L.M. Molina, M.D. Rasmussen, B. Hammer, J. Chem. Phys. 120 (2004) 7673.
[62] Z.P. Liu, X.Q. Gong, J. Kohanoff, C. Sanchez, P. Hu, Phys. Rev. Lett. 91 (2003).
[63] I.X. Green, W. Tang, M. Neurock, J.R. Yates, Science 333 (2011) 736.
[64] K.S. Kim, M. Barteau, Surf. Sci. 223 (1989) 13.
[65] C.Y. Wang, H. Groenzin, M.J. Shultz, J. Phys. Chem. B 108 (2004) 265.
[66] M. Badlani, I.E. Wachs, Catal. Lett. 75 (2001) 137.
[67] M.A. Henderson, S. Otero-Tapia, M.E. Castro, Faraday Discuss. 114 (1999) 313.
[68] E. Farfan-Arribas, R.J. Madix, Surf. Sci. 544 (2003) 241.
[69] I.E. Wachs, R.J. Madix, J. Catal. 53 (1978) 208.
[70] B.A. Sexton, A.E. Hughes, N.R. Avery, Surf. Sci. 155 (1985) 366.
[71] W.S. Sim, P. Gardner, D.A. King, J. Phys. Chem. 99 (1995) 16002.
[72] J.N. Russell, S.M. Gates, J.T. Yates, Surf. Sci. 163 (1985) 516.
[73] I.E. Wachs, R.J. Madix, Surf. Sci. 76 (1978) 531.
[74] D.A. Outka, R.J. Madix, Surf. Sci. 179 (1987) 351.
[75] D.A. Outka, R.J. Madix, J. Am. Chem. Soc. 109 (1987) 1708.
[76] M. Bowker, R.J. Madix, Surf. Sci. 95 (1980) 190.
[77] X.Y. Liu, R.J. Madix, C.M. Friend, Chem. Soc. Rev. 37 (2008) 2243.
[78] J.S. Spendelow, A. Wieckowski, Phys. Chem. Chem. Phys. 9 (2007) 2654.
[79] O. Ozturk, J.B. Park, T.J. Black, J.A. Rodriguez, J. Hrbek, D.A. Chen, Surf. Sci. 602 (2008) 3077.

[80] K. Varazo, F.W. Parsons, S. Ma, D.A. Chen, J. Phys. Chem. B 108 (2004) 18274.
[81] S.A. Tenney, J.S. Ratliff, W. He, C.C. Roberts, S.C. Ammal, A. Heyden, D.A. Chen, J. Phys. Chem. C 114 (2010) 21652.
[82] J.B. Park, J.S. Ratliff, S. Ma, D.A. Chen, J. Phys. Chem. C 111 (2007) 2165.
[83] J. Zhou, S. Ma, Y.C. Kang, D.A. Chen, J. Phys. Chem. B 108 (2004) 11633.
[84] J.B. Park, S.F. Conner, D.A. Chen, J. Phys. Chem. C 112 (2008) 5490.
[85] A. Illingworth, J. Zhou, O. Ozturk, D.A. Chen, J. Vac. Sci. Technol. B 22 (2004) 2552.
[86] J.G. Serafin, C.M. Friend, J. Am. Chem. Soc. 111 (1989) 8967.
[87] S. Ma, J. Zhou, Y.C. Kang, J.E. Reddic, D.A. Chen, Langmuir 20 (2004) 9686.
[88] L. Lin, B.R. Quezada, P.C. Stair, J. Phys. Chem. C 114 (2010) 17105.
[89] S.E. Stein, NIST Standard Reference Database Number 69: NIST Chemistry Webbook, National Institute of Standards and Technology (NIST), 2011.
[90] D.A. Chen, C.M. Friend, J. Phys. Chem. 100 (1996) 17640.
[91] D.A. Chen, C.M. Friend, Langmuir 14 (1998) 1451.
[92] X.P. Xu, C.M. Friend, Surf. Sci. 260 (1992) 14.
[93] B.J. Xu, X.Y. Liu, J. Haubrich, R.J. Madix, C.M. Friend, Angew. Chem. Int. Ed. 48 (2009) 4206.
[94] L. Gamble, L.S. Jung, C.T. Campbell, Surf. Sci. 348 (1996) 1.
[95] K.S. Kim, M.A. Barteau, J. Mol. Catal. 63 (1990) 103.
[96] E. Farfan-Arribas, R.J. Madix, J. Phys. Chem. B 106 (2002) 10680.
[97] J. Haubrich, E. Kaxiras, C.M. Friend, Chem. Eur. J. 17 (2011) 4496.
[98] B.J. Xu, J. Haubrich, C.G. Freyschlag, R.J. Madix, C.M. Friend, Chem. Sci. 1 (2010) 310.